Langmuir

ARTICLE

pubs.acs.org/Langmuir

Shear-Induced Disruption of Dense Nanoemulsion Gels

James N. Wilking,[†,⊥] Connie B. Chang,[†,⊥] Michael M. Fryd,[†] Lionel Porcar,[∥,#] and Thomas G. Mason*[,†,‡,§]

[†]Department of Chemistry and Biochemistry, [‡]Department of Physics and Astronomy, and [§]California NanoSystems Institute, University of California—Los Angeles, 607 Charles E. Young Drive East, Los Angeles, California 90095, United States

[∥]Center for Neutron Research, National Institute of Standards and Technology, Gaithersburg, Maryland 20899, United States

ABSTRACT: The structural evolution and rheology of dense nanoemulsion gels, which have been formed by creating strong attractions between slippery nanodroplets, are explored as a function of steady shear rate using rheological small-angle neutron scattering (rheo-SANS). For applied stresses above the yield stress of the gel, the network yields, fracturing into aggregates that break and reform as they tumble and interact in the shear flow. The average aggregate size decreases with increasing shear rate; meanwhile, droplet rearrangements within the clusters, allowed by the slippery nature of the attractive interaction, increase the local density within the aggregates. At the highest shear rates, all clusters disaggregate completely into individual droplets.

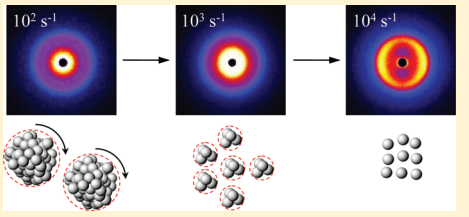

INTRODUCTION

Attractive forces between colloids can lead to multiparticle aggregates that exhibit complex responses to applied flows and osmotic stresses. Any attraction that does not cause irreversible particle aggregation in dispersions or droplet coalescence in emulsions must preserve a thin film of the continuous liquid phase between the colloids, leading to a slippery bond that is not shear-rigid. Tenuous aggregates and gels can be formed from colloids interacting through a secondary attractive well in the pair potential energy;[1,2] these are jammed nonequilibrium systems. Colloidal rearrangements and the compaction of aggregates can be induced by disturbances, such as an applied osmotic pressure or flow, so the gel's structural states are typically history-dependent. Since the attractive potential energy between particles at the secondary minimum $|U_{min}|$ can be significantly larger than the thermal energy, k_BT, flow-induced excitations that approach and exceed $|U_{min}|$ can cause droplet rearrangements within the gel, can break a gel into disconnected clusters, and can even cause the complete disruption of small clusters.

Although the influence of mechanical shear, both linear oscillatory and steady, on the structure and mechanical properties of colloidal gels has been explored over a limited range of shear strain rates $\dot{\gamma}$,[3] the understanding of the evolution of the structure of slippery aggregates in dense attractive colloidal dispersions remains incomplete. This is particularly true at the high strain rates required to disaggregate attractive clusters completely into individual droplets. At very high $\dot{\gamma}$, directly imaging the evolving structure is extremely challenging, and the complete disaggregation of spherical particles that interact through shear-rigid attractions has been observed only through light scattering from gels at low particle volume fractions ϕ.[4−6]

One way to approach this challenge and gain insight into the structural evolution of an attractive system at higher ϕ is to study a model colloidal system that creates soft gels of droplets having slippery attractions, such as nanoemulsions. Nanoemulsions are long-lived metastable dispersions of droplets of a liquid having radii $a < 100$ nm in another immiscible liquid[7] and differ from lyotropic phases known as microemulsions of swollen micelles that can have a similar size. Nanoemulsions are ideal for studying the rheology of concentrated dispersions because they can be sheared to very high $\dot{\gamma}$ without the danger of suddenly jamming and damaging a rheometer, which can occur with dense dispersions of solid particles that have very high internal moduli and nonlubricated frictional contacts. In addition, certain oil-in-water nanoemulsion systems can be remarkably stable against coalescence, even at high $\dot{\gamma}$ that could cause the disruption of attractive clusters accessible by standard rheometers, yet at much lower strain rates than those extreme strain rates used by microfluidic homogenizers to create the nanoemulsion by flow-rupturing microdroplets into nanodroplets. Consequently, for a certain known nanoemulsion composition, the nanodroplets' sizes and spherical shapes would remain largely unaffected at significant strain rates that could disrupt attractive clusters; the scattering form factor would not change because of the flow, but the structure factor could. This simplification of interpretation opens the door to studying shear-induced changes in flowing attractive nanoemulsions probed by scattering techniques, such as small-angle neutron scattering (SANS) and small-angle X-ray scattering (SAXS), that are sensitive to the droplet-scale structure.

Here, we investigate shear-induced structural and rheological changes of a strongly aggregated, dense colloidal gel built using nanoemulsions that have slippery attractive interactions between nanodroplets, controlled primarily through the ionic strength of the solution surrounding the charge-stabilized droplets. Through slippery diffusion-limited cluster aggregation (S-DLCA),[1,2] we initially form a gel of attractive nanoscale silicone oil droplets in water that interact with strong short-range bonds that are not shear-rigid. Although the salt-induced slippery attractions between the droplets are quite strong relative to the thermal energy, a highly screened, very short-range charge repulsion between the

Received: January 3, 2011
Revised: March 13, 2011
Published: April 06, 2011

droplets' interfaces (having a Debye screening length of about a nanometer) inhibits droplet coalescence. By shearing an attractive nanoemulsion over a broad range of $\dot{\gamma}$ and simultaneously probing shear stress while measuring nearest-neighbor correlations through rheological small-angle neutron scattering (rheo-SANS),[8,9] we follow the shear-induced structural changes of the gel. To show the basic behavior of a dense gel of attractive slippery droplets, we carefully examine a single $\phi = 0.44$ that is well below the point of maximal random jamming of monodisperse hard spheres (i.e., below $\phi \approx 0.64$) yet large enough that the gel network is dense and the attractive nanoemulsion's viscosity is strongly shear-thinning.

After performing rheo-SANS experiments and analyzing the results, we find that the measurements can be interpreted in terms of three different regimes of dynamic structures that depend on $\dot{\gamma}$. First, at low $\dot{\gamma}$, the gel behaves as a yield-stress solid with strongly shear-thinning viscosity, and after the initial transients have died away, the gel network breaks and reforms in a steady state. Second, at moderate $\dot{\gamma}$, the viscosity depends only weakly on $\dot{\gamma}$; the gel network is disrupted, weakens, and develops larger length scale heterogeneities as $\dot{\gamma}$ increases. Third, above a certain critical strain rate, $\dot{\gamma}_c$, the viscous stress becomes large enough to completely disrupt these locally dense clusters into individual droplets (i.e., causes the disaggregation of droplets), leading to pronounced shear-thinning behavior.[10,11] By subsequently reducing $\dot{\gamma} < \dot{\gamma}_c$, the influence of the aggregation and interdroplet attraction again becomes important, consistent with the observed thixotropy in the nanoemulsion's viscosity.

METHODS

Attractive Nanoemulsion Formation. Poly(dimethylsiloxane) (PDMS) silicone oil-in-water nanoemulsions stabilized against coalescence by the presence of an ionic surfactant, sodium dodecyl sulfate (SDS), are created by subjecting a microscale premix emulsion to extreme flow rates ($\approx 10^8$ s^{-1}) within a high-pressure stainless steel−ceramic microfluidic homogenizer. After ultracentrifugal fractionation to reduce the polydispersity, the nanoemulsions have an average droplet radius, $\langle a \rangle = 40 \pm 8$ nm, measured using SANS at dilute ϕ and confirmed with dynamic light scattering.[1,7] During fractionation, the surfactant concentration is set to $C_{SDS} = 10$ mM.

The subsequent addition of monovalent salt (NaCl) solutions, yielding final concentrations of $C_{salt} > 300$ mM, induces a strong short-range attraction between the nanoemulsion droplets.[1,12] Although the existence of the salt-induced attraction, consisting of a secondary attractive minimum that forms below a critical temperature T_c that increases with increasing C_{salt}, has been known for many years,[13] its fundamental origin and quantitative aspects remain poorly explained. The depth of this secondary minimum, $|U_{min}|$, also increases with increasing C_{salt} and can become much greater than k_BT without inducing droplet coalescence. The thin liquid film between attractive droplets provides lubrication and allows droplets to slip around one another so that they interact through strong slippery bonds that are not shear-rigid. We speculate that the origin of this attraction between droplets is similar to the one seen between charged polyelectrolytes that can cause attractions in salt solutions. Because aggregated droplets of PDMS in water at dilute ϕ are well known to cream under gravity, we choose to examine a large, $\phi = 0.44$, for which such gravitational creaming is negligible and the emulsion remains uniform.

Rheo-SANS. To study how shear influences the droplet structure, we have performed rheo-SANS measurements of attractive nanoemulsion gels over a range of scattering angles, 0.0015 Å$^{-1} \le q \le 0.02$ Å^{-1}, using neutrons of wavelength $\lambda = 8$ Å. To shear the nanoemulsion gel and measure $I(q)$ at fixed $\phi = 0.44$ and $C_{SDS} = 10$ mM simultaneously for various C_{salt} and $\dot{\gamma}$ values, a stress-controlled rheometer (Paar Physica USD200) outfitted with a custom-designed (quartz cup and rotating hollow titanium bob) concentric cylinder Couette cell[8] (gap of $h = 0.5$ mm) is positioned centrally in the neutron beam. The neutron beam is perpendicular to the rotational axis and passes directly through the center of the Couette cell, so we obtain scattering from the velocity−vorticity (x−y) plane (Figure 1c, inset). The form factor $F(q)$ is obtained from the scattered neutron intensity $I(q)$ of isolated nonattractive droplets suspended in pure D_2O at dilute $\phi = 0.005$. We set the H_2O/D_2O ratio to 48:52 for a total cell path length of $2h = 1$ mm to keep multiple scattering acceptably low while providing strong single coherent scattering.

Steady-shear rheology measurements have been performed using applied stresses that are well above the yield stress of the material; strain-rate sweeps (10^0 s$^{-1} \le \dot{\gamma} \le 10^4$ s^{-1}) have been conducted to measure the effective viscosity of the gel $\eta(\dot{\gamma})$ corresponding to $I(q, \dot{\gamma})$ simultaneously. All samples were loaded by heating the gel above the critical temperature to about 50 °C to disaggregate the droplets, pouring the hot solution into the Couette cup, inserting the bob, and then allowing the sample to cool and gel at room temperature (23 °C). Once cooled, the gel samples were disaggregated by preshearing at the highest $\dot{\gamma}$ for several minutes; the shearing was then stopped abruptly, and the dense attractive gel was allowed to reform. This was done to ensure the same shear history for all trials. Although a small amount of sample was expelled from the Couette cup during the initial preshearing step, the volume of sample in the scattering path did not change. In addition, the volume fraction of droplets in the sample did not change; this was verified by comparing the scattering intensity at high q (i.e., in the Porod regime) before and after each measurement. After experiencing the high-$\dot{\gamma}$ preshear, the sample recovered to an elastic gel state and the droplet size distribution did not change significantly. For each concurrent measurement, both the scattering and rheology were measured for at least 10 min in order to obtain adequate scattering statistics. Separate rheology-only measurements were performed using an equivalent Couette cell that has an outer rotating cup; for these measurements, the sample was subjected to the same preshear conditions described above.

Because the attraction between the droplets is temperature-dependent, it is important to ensure that any disruption is not due to temperature changes. The gel's temperature in the Couette cell can be rapidly decreased using a heating and cooling system connected to a liquid-nitrogen tank. At the highest attainable shear rate of $\dot{\gamma} = 10^4$ s^{-1}, we estimate that the viscous power dissipation per unit volume is roughly $P = \eta\dot{\gamma}^2/2 \approx 0.1$ J/(s·mL), so heating though the phase transition, even when neglecting the active thermal cooling and heat capacity of the cup and bob, would require about 20 min, which is longer than the timescale of our measurement. Thus, the effects of heating through viscous dissipation are negligible.

Because the inner cylinder (i.e., bob) of the Couette cell rotates while the outer cylinder (i.e., cup) is fixed, it is possible to create Taylor−Couette vortex flows at very high flow rates. In the Couette geometry, the instability has been shown to be fully established at a Reynolds number of $Re = 41.2(R_C/h)^{1/2}$,[8,14] where R_C is the average of the radii of the inner and outer cylinders. For our dimensions of $R_C = 2.425$ cm, the instability should occur at $Re \approx 287$. The Reynolds number in a shear flow is defined as $Re = \rho\dot{\gamma}h^2/\eta$, where ρ is the fluid density and η is the fluid viscosity. Rearranging, we find the shear rate associated with the establishment of the Taylor−Couette instability: $\dot{\gamma}_{TC} = \eta Re/\rho h^2$. For $\eta = 0.1$ P, $Re \approx 287$ and $\rho = 0.974$ g/cm^3, we find $\dot{\gamma}_{TC} = 11\,800$ s^{-1}, which is slightly above our highest $\dot{\gamma}$. Although the highest shear rates that we use are close to this threshold, even if a Taylor−Couette instability were to develop, the length scale characterizing the vortices would be similar to h and much longer than any length scale probed by SANS. Shear banding,

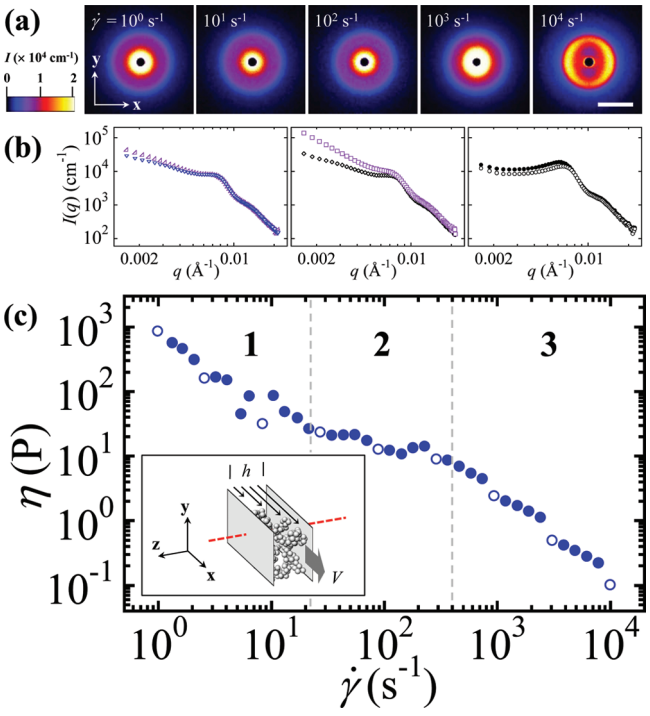

Figure 1. (a) Two-dimensional small-angle neutron scattering intensity from an attractive nanoemulsion gel, which has an average droplet radius of $\langle a \rangle = 40 \pm 8$ nm, a volume fraction of $\phi = 0.44$, and a salt concentration of $C_{salt} = 700$ mM, highlights the structural evolution of the gel as a function of the steady shear rate, $\dot{\gamma}$: from 10^0 s^{-1} to 10^4 s^{-1} in factors of 10 (left to right). The pseudocolor scale represents a linear range in scattering intensity I (0 cm^{-1} ≤ I ≤ 2.1 × 10^4 cm^{-1}). The scale bar (white) is 0.010 Å^{-1}. (b) Full (360°) azimuthal averages of the isotropic 2D scattering intensity provide the scattering intensity as a function of wavenumber $I(q)$ for $\dot{\gamma} = 10^0$ s^{-1} (open left-pointing upright triangle) and 10^1 s^{-1} (▽) (left-most plot), and for clarity, 10^2 s^{-1} (◇) and 10^3 s^{-1} (□) (center plot). There is no distinguishable difference between $I(q)$ at $\dot{\gamma} = 0$ s^{-1} (not shown) and $I(q)$ at $\dot{\gamma} = 10^0$ s^{-1} (△). Partial azimuthal averages (±10°) along the velocity (●) and vorticity (○) for $\dot{\gamma} = 10^4$ s^{-1} directions show the anisotropy in $I(q_x)$ vs $I(q_y)$ (right-most plot). (c) Steady shear viscosity η of the gel as a function of strain rate $\dot{\gamma}$. Solid circles (●) indicate steady shear measurements only (20 s duration); open circles (○) indicate steady shear measurements combined with simultaneous SANS measurements (20 min duration). Toward higher $\dot{\gamma} > 10^2$ s^{-1}, the longer duration of flow during the SANS measurements leads to noticeable downward jumps in the viscosity between solid and open circles, emphasizing the flow-history dependence. The gel exhibits two shear-thinning regimes (regimes 1 and 3) separated by a plateau in $\eta(\dot{\gamma})$ (regime 2). Gray dashed lines mark the onset of the second and third shear-thinning regions. (Inset) Neutron beam (red dashed line) intersecting the sheared gel normal to the velocity−vorticity (x−y) plane. Gelled droplets are not to scale with respect to the gap, h.

even if present at the lowest $\dot{\gamma}$ we examine, is negligible at higher $\dot{\gamma}$ where complete disaggregation occurs.[15] Minor, intermittent wall slip was observed in the first decade of $\dot{\gamma}$ (i.e., for the lowest observed $\dot{\gamma}$); however, a homogeneous flow profile was observed at higher $\dot{\gamma}$.

RESULTS AND DISCUSSION

Following the sample preparation and rheo-SANS protocols described in the Methods section (above), we have measured a series of 2D scattering patterns of an attractive silicone oil-in-water nanoemulsion at $\phi = 0.44$ over a wide range of $\dot{\gamma}$, as shown in Figure 1a. At the lowest strain rate, the nanoemulsion scatters strongly toward low q, indicating the presence of a gel network of droplets having large-length-scale features. This low-q scattering decreases through the first shear-thinning regime and into the intermediate regime. At greater strain rates, the gel enters a second shear-thinning regime, and strong scattering at low q reappears. At the largest shear rate, $\dot{\gamma} \approx 10^4$ s^{-1}, the scattering pattern changes dramatically; the scattering at low q drops abruptly, and an anisotropic ring, exhibiting a broadly smeared nearest-neighbor peak along the shear direction at higher q, emerges.

To quantify the q dependence, we azimuthally average the scattering patterns from Figure 1a and plot $I(q)$ as a function of q in Figure 1b. Scattering patterns corresponding to $\dot{\gamma} \approx 10^0$, 10^1, 10^2, and 10^3 s^{-1} are isotropic (to within 5%) and can be averaged over all azimuthal angles (360°) to obtain $I(q)$. The scattering pattern at $\dot{\gamma} = 10^4$ s^{-1} exhibits shear-induced anisotropy with a greater scattering intensity along the velocity direction. To capture this effect, we azimuthally average sectors (±10°) along the velocity and vorticity directions to obtain $I(q)$. Fluctuations in the low-q scattering with increasing $\dot{\gamma}$, which are observed in the 2D patterns, are clearly highlighted by $I(q)$; with increasing $\dot{\gamma}$, scattering toward low q first decreases, increases, and then drops dramatically at the highest $\dot{\gamma}$. In addition, a droplet−droplet nearest-neighbor correlation peak (corresponding to a ringlike feature in the SANS patterns) at higher q can also be seen at all $\dot{\gamma}$. Although the peak at the lowest $\dot{\gamma}$ is a consequence of the dense clusters containing droplets that have a significant number of nearest neighbors, which is a previously identified signature of "slippery DLCA,"[1,2] the peak observed under steady shear is less pronounced than cluster peaks seen previously with static slippery DLCA gels composed of monodisperse droplets at lower ϕ and $\dot{\gamma} = 0$ s^{-1}. The reduction in the peak height and effective smearing of the peak shape is most likely due to an increased range of nearest-neighbor distances at larger ϕ and possibly also due to a slightly larger polydispersity. This peak changes little with increasing strain rates until the highest $\dot{\gamma}$ when the peak intensity increases at a slightly lower q. This change corresponds to a drop in the low-q scattering and the appearance of anisotropy in the scattering pattern.

The gel exhibits two strong shear-thinning regimes (1 s^{-1} ≤ $\dot{\gamma}$ ≤ 2 × 10^1 s^{-1} and 4 × 10^2 s^{-1} ≤ $\dot{\gamma}$ ≤ 10^4 s^{-1}) separated by an intermediate region (2 × 10^1 s^{-1} ≤ $\dot{\gamma}$ ≤ 4 × 10^2 s^{-1}) in which η is weakly dependent on $\dot{\gamma}$ (Figure 1c). More extensive rheology-only measurements of an attractive nanoemulsion gel having identical composition and shear history are displayed in Figure 3c; these additional measurements highlight the correspondence between the rheology of the three different $\dot{\gamma}$ regimes and the microscopic structure of the gel network. At low $\dot{\gamma}$, corresponding to the first regime, the gel is strongly shear-thinning and a decrease in $I(q)$ at low q is observed. At intermediate $\dot{\gamma}$, corresponding to the second regime, there is a weak dependence of η on $\dot{\gamma}$ and $I(q)$ begins to increase at low q. At the highest $\dot{\gamma}$ that we access, a third regime is reached where the gel once again becomes strongly shear-thinning; simultaneously, $I(q)$ drops at low q, indicating the disappearance of heterogeneous attractive droplet structures over the q range that we access. Moreover, a distinctive anisotropic ring due to nearest-neighbor correlations that are stronger along the velocity direction appears and dominates the low-q scattering.

To follow the evolution of the scattering pattern clearly with increasing $\dot{\gamma}$, we azimuthally average the scattering data at each $\dot{\gamma}$ along the velocity direction (±10°), divide $I(q)$ at each $\dot{\gamma}$ by $I(q)$ at $\dot{\gamma} = 0$ s^{-1}, and plot the result as $X(q)$ in Figure 2. Because the

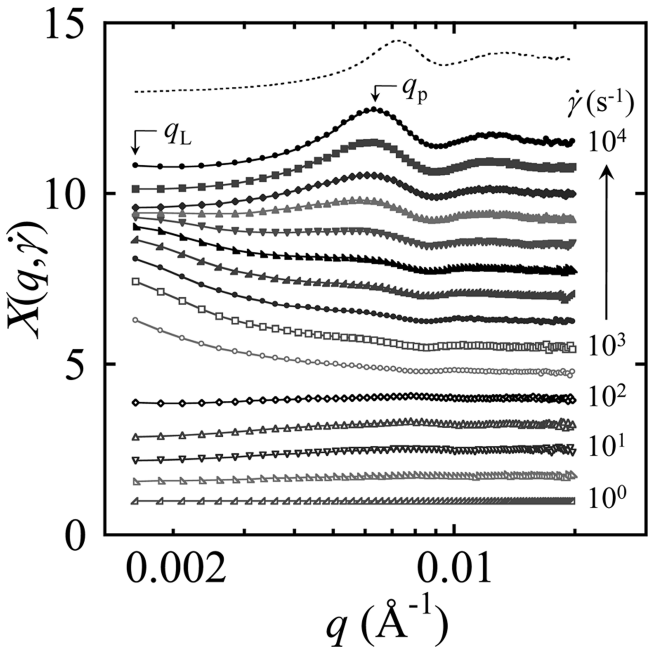

Figure 2. $I(q)$ values of the attractive nanoemulsion (Figure 1) at each $\dot{\gamma}$ are divided by $I(q)$ at $\dot{\gamma} = 0\ s^{-1}$ and plotted as a function of the wavenumber and shear rate, yielding $X(q, \dot{\gamma})$ for a series of shear rates: $\dot{\gamma} = 1$ (open left-pointing upright triangle), 2.57 (open right-pointing upright triangle), 8.38 (▽), 27.3 (△), 88.9 (◇), 289 (○), 1000 (□), 1270 (●), 1700 (solid left-pointing upright triangle), 2290 (solid right-pointing upright triangle), 3070 (▼), 4120 (▲), 5540 (♦), 7440 (■), and 10 000 (●) s^{-1}. For clarity, $X(q)$ at each successive $\dot{\gamma}$ is offset by a constant value of 0.6. The upper, black dotted line represents the normalized scattering intensity measured for an isotropic, repulsive, highly elastic nanoemulsion glass at $\dot{\gamma} = 0\ s^{-1}$ having the same $\langle a \rangle$ and ϕ and without NaCl salt. $X(q)$ for the most strongly sheared attractive gel of nanodroplets has features that are qualitatively similar to those of the static repulsive glass.

anisotropy in the scattering pattern at the highest $\dot{\gamma}$ is less than 20%, this analysis method systematically captures the primary structural changes over all $\dot{\gamma}$. Although $I(q)$ contains scattering contributions from the droplet form factor $F(q)$ in addition to the structure factor $S(q)$, at even the largest $\dot{\gamma}$ the viscous stress $\tau \approx 10^3$ dyn/cm^2 is much lower than the Laplace pressure of an individual nanoemulsion droplet, $\Pi_L \approx 10^6$ dyn/cm^2, so the droplets are essentially undeformed and changes in $F(q)$ are negligible. Therefore, $X(q, \dot{\gamma})$ highlights shear-induced changes in the droplet configurations rather than changes in droplet shape. The scattering at the lowest q that we can access represents a crossover in scattering between two length scales: large droplet aggregates (e.g., a steady-state gel network of many-droplet clusters), which effectively have larger length-scale features that scatter below the accessible q range of the SANS instrument, and the local nearest-neighbor droplet correlations, which scatter toward higher q. We infer that the normalized intensity at the lowest q we measure, denoted $X_L(\dot{\gamma})$, primarily arises from the high q power law shoulder of a correlation peak below this q-range. At higher q, the normalized intensity associated with the center of the nearest neighbor correlation peak, denoted $X_p(\dot{\gamma})$, represents scattering from correlated droplet centers separated by an average distance of $d \approx (2\pi)/q_p$. For aggregated droplets, $d \approx 2a$ and $q_p \approx 0.0078$ Å^{-1}. However, at such low $\dot{\gamma}$, this peak is not the dominant scattering feature (Figure 1b). Changes in the peak position as a function of $\dot{\gamma}$ are obscured until $\dot{\gamma} \geq 10^3\ s^{-1}$, where a peak can be distinguished at $q_p \approx 0.006$ Å^{-1} (Figure 2). This emerging peak corresponds to average droplet separations of $d \approx 100$ nm, slightly larger than the droplet diameter, corresponding to attractive droplets that are nearly touching one or more neighboring droplets. For comparison, we have measured $I(q)$ of a repulsive nanoemulsion having the same ϕ and size distribution yet no added NaCl, and in the uppermost part of Figure 2, we plot the q-dependent intensity of the zero-salt nanoemulsion, normalized by the intensity from the high-salt nanoemulsion, both at $\dot{\gamma} = 0\ s^{-1}$. The correlation peak of the repulsive nanoemulsion at $q \approx 0.007$ Å^{-1} is quite close to that of the attractive nanoemulsion at the highest $\dot{\gamma} = 10^4\ s^{-1}$, and qualitatively, the features are very similar.[16]

Although the viscosity drops dramatically in the first decade of $\dot{\gamma}$ (Figure 1c), the corresponding structural changes occur on length scales longer than we can access through SANS. The first two decades in $\dot{\gamma}$ provide no measurable change in $X_p(\dot{\gamma})$, but $X_L(\dot{\gamma})$ decreases slightly (Figure 2). This drop in $X_L(\dot{\gamma})$ at low $\dot{\gamma}$ is consistent with a steady-state dynamic gel network in which the bonds between clusters of droplets are continuously being formed and broken by the slow, steady shear. Under the influence of the steady shear, the kinetically arrested gel network fractures into a dense array of many transient clusters that have a tendency to tumble yet still attractively interact with each other while being sheared. As bonds are broken between clusters, other bonds between neighboring clusters are formed, causing the average steady-shear structure to reflect an increase in the length scale associated with the larger-scale heterogeneities in the attractive gel structure. The slow flow appears to cause the gel's larger-scale heterogeneities to become even larger, thereby shifting the tail of the scattering intensity associated with these heterogeneities to values of q that are below our accessible measurement window, so $X_L(\dot{\gamma})$ decreases. At this high ϕ and low $\dot{\gamma}$, the gel is a dynamic network that anneals as it slowly breaks and reforms, so droplet clusters can be imagined as being a part of a steady-state network in which bonds between neighboring clusters are continuously being formed and broken. At these low strain rates, there is little change in the high-q droplet correlation peak at $X_p \approx 1$, indicating that the local droplet structure remains relatively unchanged and that the attraction between individual particles still dominates the hydrodynamic forces. The plateau in viscosity at intermediate strain rates ($30\ s^{-1} \leq \dot{\gamma} \leq 300\ s^{-1}$) is reminiscent of the rheological behavior of attractive microscale emulsions that exhibit a vorticity alignment of droplet clusters. The alignment of such clusters, if present here, would occur at large length scales inaccessible with SANS and would scatter well below our q range.

In Figure 3, we plot the changes in the primary scattering features for the highest two decades of $\dot{\gamma}$ that we examine, $X_p(\dot{\gamma})$ and $X_L(\dot{\gamma})$, in Figure 3a,b, respectively. The most dramatic structural changes occur between $\dot{\gamma} \approx 10^3$ and $10^4\ s^{-1}$; within one decade in $\dot{\gamma}$, a 2-fold increase in $X_p(\dot{\gamma})$ is accompanied by a 3-fold drop in $X_L(\dot{\gamma})$. At the highest $\dot{\gamma}$, the reduction in X_L and the increase in X_p indicate that a majority of droplets have become disaggregated, and X_p exceeds the intensity of the correlation peak for a glassy system of purely repulsive droplets with an average of nearest neighbors of $z \approx 6$. This suggests the presence of a more ordered, shear-induced structure having $z > 6$.[17] This is consistent with the observation that the correlation peak for shear-induced disaggregated droplets is slightly lower in q than in the purely repulsive case. A 3-fold increase in $X_L(\dot{\gamma})$ between $\dot{\gamma} \approx 10^2$ and $10^3\ s^{-1}$ is indicative of the disruption of the gel into a distribution of cluster sizes in which the average cluster size decreases as the shear rate increases. As scattering

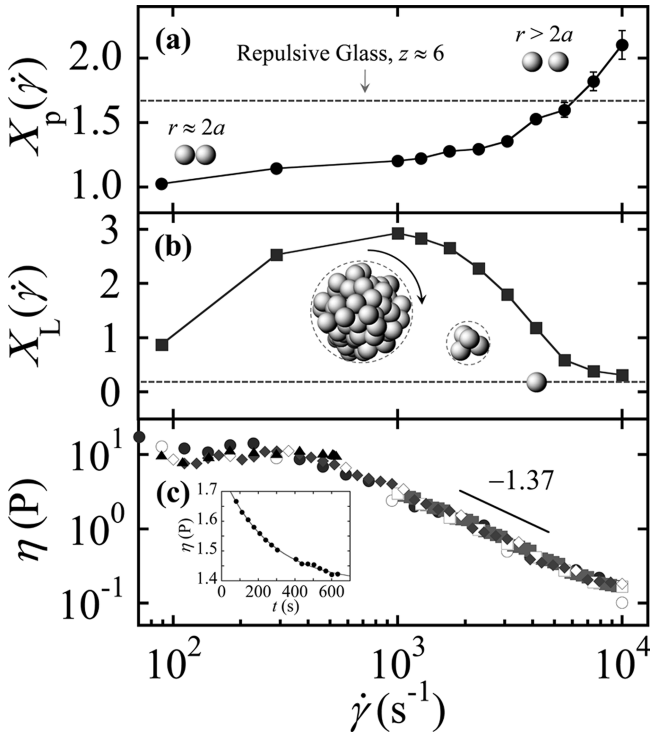

Figure 3. Primary features of the normalized scattering function $X(\dot{\gamma})$ highlight the structural evolution and disaggregation of the attractive nanoemulsion at high $\dot{\gamma}$. (a) $X_p(\dot{\gamma})$ represents the intensity of the nearest-neighbor correlation peak (centered at $q \approx 0.006$ Å^{-1}) relative to the zero-shear intensity; X_p becomes the dominant SANS feature at high $\dot{\gamma}$. The dashed line represents the normalized intensity at q corresponding to the nearest-neighbor correlation peak, $X_{p,glass}$, for the isotropic, repulsive nanoemulsion glass described in Figure 2. (b) $X_L(\dot{\gamma})$ represents the normalized scattering intensity at the lowest q of our SANS measurement. The dashed line represents X_L for a purely repulsive nanoemulsion glass. (c) Measurements of the steady shear viscosity $\eta(\dot{\gamma})$ for an identical nanoemulsion. Here, $\dot{\gamma}$ has been swept in both directions: from low to high (● and ■) and from high to low (▲ and ♦). Filled symbols represent rheology-only measurements; open symbols indicate simultaneous rheological and neutron-scattering measurements. The total measurement times associated with the open symbols are 20 (○), 10 (□), and 5 (◊) minutes. The solid line at high q represents a power law shear-thinning behavior having an exponent of 1.37, which is more extreme than the exponent of unity that corresponds to classical shear-thinning behavior of a yield-stress solid. (Inset) Separate rheology-only measurement of η as a function of time for an attractive nanoemulsion gel (C_{salt} = 700 mM, ϕ = 0.44) after an abrupt jump in shear rate from 10^2 to 10^3 s^{-1}. The decrease in viscosity is fit to an exponential decay, providing a characteristic time of ∼260 s.

from the cluster distribution approaches our lower limit in q, the high-q shoulder and tail of the scattering from smaller-scale attractive heterogeneities in the flowing nanoemulsion begin to extend into our SANS q range, resulting in an increase in $X_L(\dot{\gamma})$. $X_p(\dot{\gamma})$ rises only very slightly across this range in $\dot{\gamma}$, indicating that the majority of the droplets have about the same number of nearest neighbors locally within the clusters of attractive droplets.

Four independent strain sweeps are overlaid in Figure 3c. In general, the shear-thinning behavior is reproducible and reversible, whereas at a specific $\dot{\gamma}$, η is time-dependent (i.e., thixotropic). The reproducibility of the $\dot{\gamma}$ dependence indicates that the structure is reproducible if subjected to a controlled shear history. The thixotropy implies that, at a given $\dot{\gamma}$, the system requires time to reach a steady-state evolving structure that effectively has time-independent bulk material properties. Separate rheology-only measurements of the time-dependent viscosity $\eta(t)$ demonstrate that η drops exponentially to a saturation value following an abrupt increase in the shear rate. Though the representative measurement of $\eta(t)$ plotted in the Figure 3c inset does not reach full saturation, the fit provides a measure of the characteristic time of ∼4.3 min. Because our rheo-SANS measurements have been averaged over times (20 min) much longer than those required to reach a steady state (4.3 min), our scattering data are dominated by the steady-state structure of the attractive nanoemulsion at a given shear rate after the structure has readjusted to a new flow rate.

In the $\dot{\gamma}$-range corresponding to the most dramatic changes in the scattering, the attractive nanoemulsion exhibits extreme shear thinning, where $\eta \propto \dot{\gamma}^{-\alpha}$ and we observe $\alpha > 1$ (Figure 3c). Over the range of 5×10^2 s$^{-1} < \dot{\gamma} < 10^4$ s^{-1}, we find that the shear-thinning exponent is $\alpha \approx 1.37$. For comparison, the classic shear-thinning exponent of a common yield stress material is $\alpha \approx 1$. Observing $\alpha > 1$, even over a limited range of $\dot{\gamma}$, in the sheared attractive nanoemulsion indicates the strong likelihood of an instability in the transient network structure and can be understood in light of a decrease in the effective volume fraction, which is defined as follows. In the limit of $\dot{\gamma}$ that induces complete disaggregation, the effective volume fraction occupied by all clusters as they are spun about their centers of mass, denoted ϕ_{clust}, tends toward ϕ and the viscosity drops. Calculating and comparing the viscosity for a suspension of concentrated disordered hard spheres[18] at $\phi \approx 0.64$ and 0.44 provides a factor of ∼100 with respect to the drop in the viscosity. Although this approximation is simplistic, it provides the correct order of magnitude for the drop in η that is experimentally observed.

The drop in $X_L(\dot{\gamma})$ can be potentially explained using a geometric packing constraint argument. As $\dot{\gamma}$ increases, one might expect a *decrease* in the average cluster size and a corresponding *increase* in the number of smaller clusters. These trends would contribute to a continued increase in X_L with increasing $\dot{\gamma}$ until the cluster radius is $R \approx \pi/q_L < 5a$, when the cluster peak would enter our observable range of q. Realistically, the colloidal aggregates would be inhibited from tumbling without disruption in a shear flow if ϕ_{clust} becomes large enough (e.g., beyond a jamming limit ≈0.64 for a disordered system of uniform spherical clusters) that droplets within the tumbling clusters would effectively collide. The excluded volume and the limited compressibility of the clusters preclude a narrow size distribution from systematically shifting to smaller size all the way down to the single droplet level (e.g., tetramers → trimers → dimers → single droplets).

We illustrate the essential elements of this idea through an example focused on an ensemble of attractive tetrahedral clusters composed of N = 4 monodisperse droplets in a uniform shear field. In a dilute cluster limit, the tumbling clusters are spaced far apart and would be driven to rotate in the same sense, following Jeffery orbits,[19] by the shear flow; at very dilute ϕ, viscous interactions between the rotating clusters would not be strong. However, at more concentrated ϕ, the tumbling clusters would have increasingly significant viscous interactions; as the density of clusters increases, the idealization of Jeffery orbits of isolated clusters rotating in the same direction would tend to become problematic because the local flows of the continuous viscous liquid at the outer boundary regions of neighboring tumbling clusters would be in *opposite* directions as a result of the rotations. Such strong opposing flows at the local boundaries between tumbling clusters, if present, could potentially generate much

higher local flow rates that might disrupt the internal attractive jamming of droplets within the clusters themselves. The volume fraction of droplets within a sphere of radius R that is swept out by a tumbling cluster is defined as $\phi_R = Na^3/R^3$. For a tetrahedron, the sphere of radius $R = 2.22a$ traced out by the rounded "vertices" of the cluster provides $\phi_R = 0.36$. The true droplet volume fraction is approximately $\phi \approx \phi_R\phi_{clust}$. If we assume that all droplets are aggregated in the form of tetrahedra and that tumbling clusters will collide at $\phi_{clust} \approx \phi_{RCP} \approx 0.64$, then the droplet volume fraction below which tetrahedra can tumble freely will be $\phi \approx 0.23$. From this example, it can be seen then that a monodisperse suspension of tetramers, or any very small cluster size, tumbling under shear is not realistic at $\phi = 0.44$ and that the approach to complete disaggregation must be accompanied by a broadening of the cluster size distribution or must occur at an average cluster size well above that of a tetramer. This is consistent with our SANS observation that a clearly defined cluster−cluster correlation peak is never observed at low q, even at high $\dot{\gamma}$.

Tumbling clusters of droplets in the shear flow can be dispersed into individual droplets if the applied viscous disruptive stress acting on a cluster can effectively break all of the attractive bonds in that cluster. In a very simplified model, we assume that randomly oriented compact clusters, each having N droplets and n attractive bonds, tumble in Jeffery orbits. Each cluster effectively sweeps out a volume of a sphere that is given by the radius R representing the distance from the center of the cluster to its outermost droplet's surface (Figure 3b; dashed circle). Using the Stokes−Debye relation, we crudely estimate the torque on a cluster to be $T \approx 8\pi R^3\eta\omega$, where ω represents the angular frequency of the rotation of the cluster. If each bond in the cluster has an attractive energy $|U_{min}|$, then we hypothesize that the rotational torque (which provides a rough estimate of the disruptive viscous energy per cluster due to the local opposing flows of neighboring clusters that tumble) must exceed $n|U_{min}|$ in order for all internal slippery bonds to be broken and the cluster to break up into individual droplets. On the basis of this concept, we can estimate the frequency of rotation required for cluster breakup to be $\omega_{break} \approx n|U_{min}|/8\pi R^3\eta$. Here, η represents the effective viscosity of the medium outside of a cluster and η is typically close to the viscosity of the continuous phase.

Although, as discussed previously, the effective distribution of cluster sizes (i.e., structural heterogeneities in the gel) evolves with shear rate, for sufficiently large ϕ, an ensemble of tumbling clusters may experience strong disruptive local strain rates in the lubricating liquid between neighboring clusters and even elastic collisions between the fundamental objects in the clusters. In the final stage of shear-induced disaggregation, we consider the $\dot{\gamma}$ required to disaggregate an ensemble of tumbling tetramers, so $R \approx 2.22a$, $N \approx 4$, and $n \approx 6$. We assume that the cluster distribution is at high enough ϕ_R so that a tetramer frequently encounters neighboring tetramers as it rotates, causing frequent collisions between adjacent clusters. Because $|U_{min}|$ is not known precisely for the particular interdroplet attraction induced by SDS and NaCl that we have used but is obviously significantly larger than k_BT, we assume that $|U_{min}| \approx 10k_BT$, yielding $\omega_{break} \approx 2 \times 10^4$ rad/s corresponding to $\dot{\gamma} = \omega/2\pi \approx 3 \times 10^3\ s^{-1}$ for $\eta = 1$ cP. Admittedly, although the many assumptions of this simple model need to be more fully explored, the model does provide the proper order of magnitude to explain the observation of the apparent disaggregation of droplets in attractive nanoemulsions at high $\dot{\gamma}$. A quantitative understanding would require a better knowledge of the cluster size distribution and how it evolves as a function of $\dot{\gamma}$. Although simplistic, this model of disaggregation is quite general and could also potentially be used to explain the breakup of clusters of attractive solid particles bound in secondary minima. By refining and applying this approach in reverse, structural measurements of the shear-induced disruption of attractive gels of colloids could potentially be used to determine an average $|U_{min}|$ between the basic constituent particles or droplets.

As an alternative real-space hypothesis, the observed $X(q,\dot{\gamma})$ could potentially result from very large, compacted, oblong clusters of droplets oriented with their long axes along the vorticity direction that rotate in the flow, separated by lubricating regions of continuous phase liquid. Local compaction within these dense clusters could lead to a scattering structure factor that resembles a repulsive glass and possesses anisotropy. Although this hypothesis is not consistent with our observation that the nearest neighbor correlation peaks shift to lower q at the highest strain rate, the observed peak shift is small enough that further study would be required to rule out alternative explanations such as this one completely.

CONCLUSIONS

We have explored the structural evolution and disaggregation of a dense, slippery nanoemulsion gel under the influence of steady shear using rheo-SANS. We find a decrease in scattering from droplet aggregates and the emergence of a dominant droplet−droplet correlation peak corresponding to $d > 2a$ toward higher $\dot{\gamma}$. In one possible explanation of our observations, high shear flow causes a disruption of dense clusters within the gel into individual droplets. The $\dot{\gamma}$ dependence of the scattering behavior at low q can be understood in light of a high effective volume fraction created by tumbling aggregates. The disruption of dense tumbling clusters is marked by extreme shear-thinning behavior, which is consistent with a decrease in the effective volume fraction with increasing $\dot{\gamma}$. Using a simple model of tumbling clusters that strongly interact at high densities, we estimate the $\dot{\gamma}$ required to disaggregate the smallest dense cluster, the tetramer, and this $\dot{\gamma}$ is roughly consistent with our observations.

In the future, it would be useful to repeat these measurements at lower ϕ for attractive, density-matched nanoemulsions where the effective volume fraction of the clusters is reduced. Rheo-ultra-SANS or optical scattering could be used to probe the structure of larger-scale features at lower q as a function of $\dot{\gamma}$. In addition, it would be interesting to perform similar measurements with dense gels that are built using attractive, shear-rigid bonds rather than slippery bonds to observe how the system evolves as small tumbling clusters collide at high ϕ.

AUTHOR INFORMATION

Corresponding Author

*E-mail: mason@chem.ucla.edu.

Present Addresses

[⊥]School of Engineering and Applied Sciences, Harvard University, Cambridge, Massachusetts 02138, United States.

[#]Institute Laue-Langevin, BP 156, F-38042 Grenoble, Cedex 9, France.

ACKNOWLEDGMENT

We thank Jung-Ren Huang for useful discussions. We thank NIST for neutron scattering beam time necessary to perform these rheo-SANS experiments.

REFERENCES

(1) Wilking, J. N.; Graves, S. M.; Chang, C. B.; Meleson, K.; Lin, M. Y.; Mason, T. G. *Phys. Rev. Lett.* **2006**, *96*, 015501.
(2) Seager, C. R.; Mason, T. G. *Phys. Rev. E* **2007**, *75*, 011406.
(3) Montesi, A.; Pena, A. A.; Pasquali, M. *Phys. Rev. Lett.* **2004**, *92*, 058303.
(4) Pignon, F.; Magnin, A.; Piau, J. M. *Phys. Rev. Lett.* **1997**, *79*, 4689–4692.
(5) Sonntag, R. C.; Russel, W. B. *J. Colloid Interface Sci.* **1986**, *113*, 399–413.
(6) Sonntag, R. C.; Russel, W. B. *J. Colloid Interface Sci.* **1987**, *115*, 378–389.
(7) Mason, T. G.; Wilking, J. N.; Meleson, K.; Chang, C. B.; Graves, S. M. *J. Phys.: Condens. Matter* **2006**, *18*, R635–R666.
(8) Porcar, L.; Hamilton, W. A.; Butler, P. D.; Warr, G. G. *Rev. Sci. Instrum.* **2002**, *73*, 2345–2354.
(9) Porcar, L.; Warr, G. G.; Hamilton, W. A.; Butler, P. D. *Phys. Rev. Lett.* **2005**, *95*, 078302.
(10) Doi, M.; Edwards, S. F. *J. Chem. Soc., Faraday Trans. 2* **1979**, *75*, 38–54.
(11) Goddard, J. D. *Annu. Rev. Fluid Mech.* **2003**, *35*, 113–133.
(12) Bibette, J.; Mason, T. G.; Hu, G.; Weitz, D. A.; Poulin, P. *Langmuir* **1993**, *9*, 3352–3356.
(13) Aronson, M. P.; Princen, H. M. *Nature* **1980**, *286*, 370–372.
(14) Taylor, G. I. *Philos. Trans. R. Soc. London, Sect. A* **1923**, *223*, 289–343.
(15) Mason, T. G.; Rai, P. K. *J. Rheol.* **2003**, *47*, 513–533.
(16) Wilking, J. N.; Mason, T. G. *Phys. Rev. E* **2007**, *75*, 041407.
(17) Larson, R. G. *The Structure and Rheology of Complex Fluids*; Oxford University Press: New York, 1999.
(18) Krieger, I. M.; Dougherty, T. J. *Trans. Soc. Rheol.* **1959**, *3*, 137–152.
(19) Jeffery, G. B. *Proc. R. Soc. London, Sect. A* **1922**, *102*, 161–179.